

Ultrasound Doppler technique for the diagnosis of focal nodular hyperplasia – case series and systematic review

Mikael Sawatzki¹, Thomas Burkart², Stephan Baumeler¹, David Semela¹, Yi Dong³, Christian Jenssen⁴, David Srivastava^{2,5}, Christoph F. Dietrich²

¹Division of Gastroenterology and Hepatology, Kantonsspital St. Gallen, St. Gallen, Switzerland, ²Department for Internal Medicine, Clinics Hirslanden Beau-Site, Salem and Permanence, Bern, Switzerland, ³Department of Ultrasound, Xinhua Hospital Affiliated to Shanghai Jiaotong University School of Medicine, Shanghai, China, ⁴Krankenhaus Märkisch-Oderland, Department of Internal Medicine, Strausberg, Germany, Brandenburg Institute for Clinical Ultrasound (BICUS) at Medical University Brandenburg, Neuruppin, Germany, ⁵Inselspital, University Hospital of Bern, Switzerland

Abstract

With the Superb Micro-Vascular Imaging (SMI), the established Doppler technology has been extended by another mode. With this technique, microvascular structures with slow blood flow can now also be displayed in real time. As with the introduction of Doppler ultrasound, this new technique opens further diagnostic fields for the examiner, which were previously reserved for magnetic resonance imaging (MRI), computed tomography (CT) or contrast ultrasound (CEUS). Focal nodular hyperplasia (FNH) of the liver is characterized by a typical spoke-wheel vascular malformation (spoke-wheel sign, SWS) and a good example using SMI for the diagnostic profit of our patients. The aim of this report is to describe the use of SMI as a new non-invasive, quick, and probably cost-effective diagnostic imaging tool.

Keywords: liver; ultrasound; focal nodular hyperplasia; contrast enhanced ultrasound; Color Doppler; superb micro-vascular imaging

Introduction

Doppler ultrasound (US) has been used routinely in various areas of medicine for more than fifty years [1,2]. From angiology to cardiology, gynaecology to gastroenterology and hepatology, Doppler technology found its way into the everyday medical routine and into current guidelines [3-5]. A disadvantage was always the insufficient visualisation of small vessels with slow blood flow. The subtle Doppler signals are superimposed by the body's own movement artefacts such as respiration and

heartbeat (clutter) and therefore beyond a reliable visualisation [6-8]. With the introduction of contrast enhanced ultrasound (CEUS) and with the new generation of contrast media (SonoVue[®] 2001), also small vessels became visible [3-5,9-14]. Now this evolution is continued with the development of sensitive Doppler techniques, here with superb micro-vascular imaging (SMI) by Canon (formerly Toshiba). The SMI mode now allows the visualisation of slow blood flow in small vessels with the use of a contrast agent.

Introduction into Superb Microvascular Imaging (SMI)

The principle behind SMI

In conventional Doppler, there is an overlap in the visualisation of slow blood flow and simultaneous tissue movement (clutter). To reduce these motion artifacts, the conventional Doppler uses a one-dimensional wall filter. However, this results in a reduced visualisation of the slow flow signals (fig 1). In SMI, the tissue move-

Received 24.08.2023 Accepted 08.10.2023

Med Ultrason

2023;0 Online first, 1-11

Corresponding author: Christoph F Dietrich

Department Allgemeine Innere Medizin (DAIM),
Kliniken Hirslanden Beau Site, Salem und
Permanence; Beau Site: Schänzlihalde 11,
CH-3013 Bern Switzerland
Phone: +41764408150
E-mail: ChristophFrank.Dietrich@hirslanden.ch

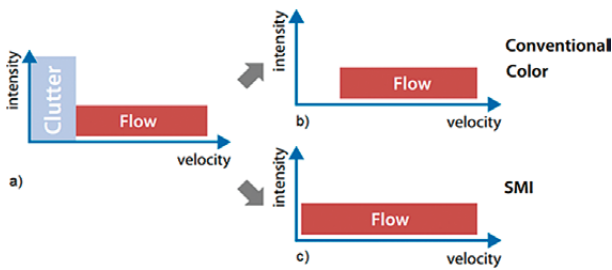


Fig 1. Schematic illustration of the SMI algorithm. In conventional Doppler, tissue movements (clutter) overlap with slow blood flow (a). With conventional Doppler, one-dimensional wall filter (line) is used, which also leads to a reduced visualization of slow blood flow (b). In SMI mode, multidimensional filter is applied, preserving the signals of slow blood flow (c). Adapted after Hata J (2014) “Seeing the unseen new techniques in vascular imaging” with permission of Toshiba Medical Systems Corporation[©] [16].

ments are analyzed with an adaptive algorithm and then the movement artifacts are removed with a multidimensional filter, which also allows to show the slow blood flow [15,16].

Color and monochrome SMI (cSMI und mSMI)

Two modes can be used within SMI. In colour mode (cSMI) grayscale and colour information are simultaneously displayed. In the monochrome mode (mSMI) the focus lies on the pure visualisation of the vessel structures. The sensitivity of the vessel image is increased by the exclusive visualisation of the grey scale with subtraction of the background information (fig 2). Furthermore, the time smoothing function (also known as frame averaging) on a scale of 1-7 can be set manually [8,17]. By increasing the scale, the flow signals are accumulated frame by frame. This allows to visualize the continuity of the vessels more accurately [15].

Image optimization

As in conventional Doppler, the US picture can be improved in SMI with several parameters. The sensitivity of the flow signal can be improved by increasing the

color gain [8,17,18]. The reduction of the region of interest (ROI) also improves sensitivity. An increase in ROI, on the other hand, results in a reduction of the frame rate. Park et al therefore recommend a reduction of the ROI to less than 2.5 cm for an optimal display [15]. However, if the color gain is increased too much while the ROI is reduced at the same time, so-called flash artifacts can occur [19,20]. For an optimal result, color gain and ROI are fine-tuned in a way that just no flash artifacts appear anymore. Another factor is the level of depth of the ROI. The deeper it lies, the longer the echoes need for the way there and back. Thus, small and superficial ROI produce better image results. To avoid motion artifacts, the patient should be asked to hold his breath. Furthermore, applying not too much pressure on the tissue prevents the vessels from collapsing, especially in the case of superficial ROI [15,21]. In our experience, microcalcifications can also cause signal artefacts, sometimes difficult to distinguish from vessels in small structures such as gallbladder polyps [22-25]. In this case, the observation of pulse-synchronous flow patterns can help to identify true vessels.

Overview of existing publications

The publications on the subject of SMI are limited so far, which is no surprise for a new imaging tool. A literature search in PubMed (June 2023) shows 87 articles published so far. However, analysis of the last years suggests that this number will rise in the next few years. A more detailed analysis until 2020 shows the following indications. Female breast (n=11) [15,26-35] followed by thyroid diagnostics (n=8) [36-43] and larger vessels (n=8) [44-52], arthritis (n=5) [53-57] and focal liver lesions (n=5) [52,58-62]. Most (n=40) publications compared SMI to another examination method such as Doppler or CEUS. Furthermore, there are 3 (5%) case-control studies, one cohort study, 8 (13%) case series and 7 (11%) case reports. Finally, there is one review article each on breast and thyroid [15,36]. Randomized controlled trials (RCT) are still lacking.

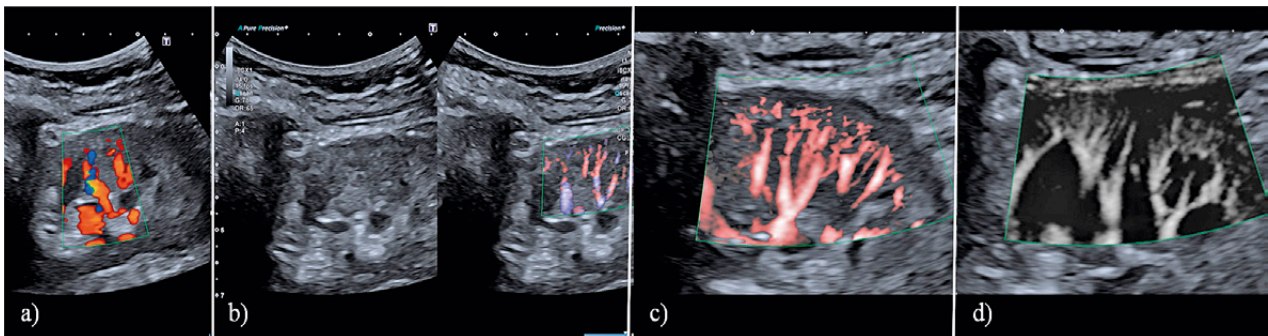


Fig 2. Kidney cortex using different display modes. Color Doppler (a). Advanced Dynamic Flow mode (b). Color SMI (cSMI) (c). Monochrome SMI (mSMI) (d).

Hypervascular focal liver lesion (FLL) using SMI, Focal Nodular Hyperplasia (FNH)

Epidemiology

Focal nodular hyperplasia (FNH) is the second most common benign liver tumor after hemangioma [7,14,63,64]. The prevalence varies depending on the source from 0.4% to 3% and accounts for about 8% of all primary liver tumors [65-68]. Although FNH is found in men and women, it most commonly affects women between 30 and 50 years with a woman-to-man ratio from 8:1 to 12:1 [68-70]. Occasionally FNH are found in children as well and CEUS and elastography are applied [14,71-78]. Bouyn et al described in children a prevalence of 0.02% based on 11000 liver sonographies [79]. In most cases FNH occur solitary, but in up to 20-30% of cases occurrence is multiple and often combined with other FLL [65,68,70,80]. Multiple FNH are sometimes observed in a specific clinical context. This includes Budd-Chiari syndrome [81-83], obliterative portal venopathy [84,85] and congenital disorders such as hereditary haemorrhagic telangiectasia and portal vein agenesis [14,86]. FNH also appear in 20% together with liver hemangiomas [70,87,88]. On the other hand, neither pregnancy nor oral contraceptives are associated with the occurrence of FNH [89-95].

Clinical symptoms and natural course

In case series, it has been shown that the size of FNH usually remains stable over many years, causes no symptoms and almost no complications [89,96]. In up to 30% of patients elevated liver enzymes are observed [97]. The α -fetoprotein is typically not elevated. Other symptoms are uncommon: palpable abdominal mass in 2-4% of cases, hepatomegaly and fever in <1% of the cases [70,98,99]. Since the FNH represents a benign condition, a conservative approach can be chosen in most cases. Even in symptomatic patients, the indication for resection should be considered cautiously, as there is

only a poor correlation between FNH and symptoms [100]. Resection of the FNH is only recommended in exceptional circumstances such as pediculate lesions, exophytic growth or increase in size. On the other hand, non-surgical treatment methods should only be chosen when the patient is not operable. In case of confirmed diagnosis and asymptomatic patients no follow-up is recommended. In addition, oral contraceptives do not have to be stopped and follow-up during pregnancy is not necessary [65,101,102].

Histology and pathogenesis

The generally accepted hypothesis for the development of FNH postulates a local hyperperfusion or hypoxia at the site of an arterial malformation. This hemodynamic instability leads to local polyclonal hyperplasia of the hepatocytes [14,68,98]. This hypothesis is supported by the fact that patients with FNH also have a higher incidence of hemangioma [80,83,88]. A second indication is that in families with hereditary haemorrhagic telangiectasia, an autosomal-dominant genetic disorder characterized by vascular malformations, FNH also occurs more frequently [14,103].

FNH is typically described as an unencapsulated nodule with a central fibrotic scar in up to 70 % with dystrophic arteries [3-5,92,104]. From the center several septa usually grow radially. In various degrees, ductular proliferations and inflammatory cells can also be seen in these septa. The characteristic feature is a central feeding artery that branches to the periphery and centrifugally perfuses the nodule (fig 3, fig 4).

Furthermore, the FNH shows atypical portal veins [92,93,97]. Molecular studies showed an upregulation of extracellular matrix genes. They are associated with an activation of the transforming growth factor beta (TGF- β) and an overexpression of Wnt/ β catenin target genes coding for glutamine synthesis [107]. This β -catenin activation without β -catenin-activating mutations leads to a map-like pattern of glutamine synthase overexpression in

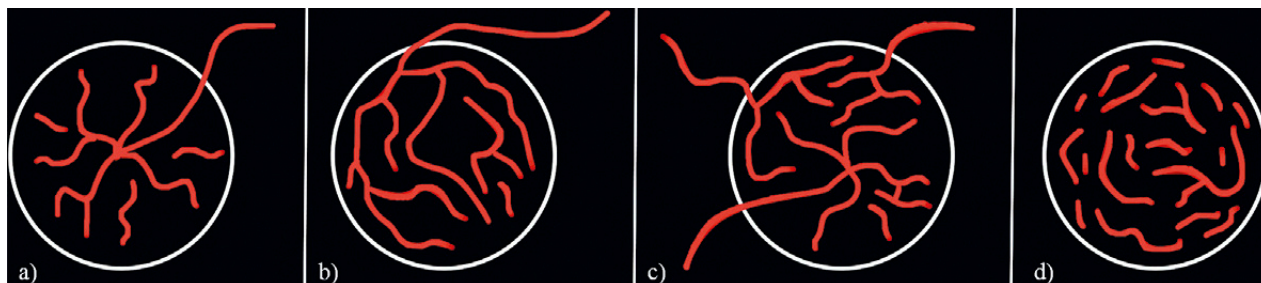


Fig 3. Classification of FNH by CEUS [14,97,105]. Type I (85%): classical type with spoke-wheel sign (SWS). Vessels run to the center using colour coded doppler ultrasound with or without a central scar (a). In the eccentric type II the central point of the vessel star is shifted to the edge. Type III (15%): Teleangiectatic “atypical” FNH, peliotic sinusoid (b) [106]. Type IV shows homogenous enhancement.

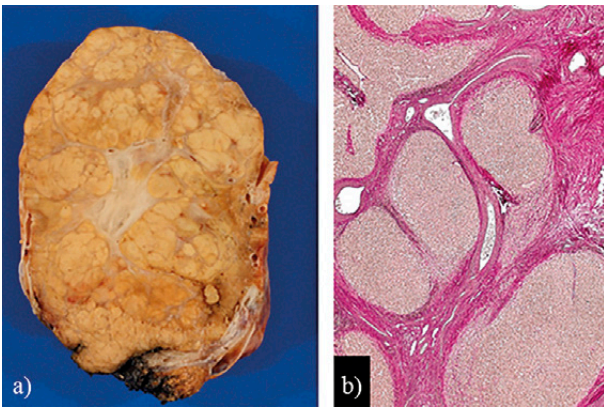


Fig 4. Resected FNH showing a central fibrotic artery (red arrow) (a). Histopathological analysis demonstrated fibrous and thickened walls of the blood vessels (Elastica-van-Gieson stain) (b).

the perivenous areas of the nodules, which is characteristic for FNH [108,109]. This characteristic feature can be used for histopathological diagnosis in difficult cases [65,110,111].

Imaging

The image properties of FNH are very similar to the underlying histopathological abnormalities in all diagnostic modalities [65]. US including CEUS, contrast enhanced CT or contrast enhanced MRI are used for diagnostic purposes. In the current EASL Guidelines, the typical features regardless of the imaging modality are summarized as follows: 1) lesion homogeneity except the central scar, 2) slightly different from the adjacent liver on pre-contrast US, CT or MRI, 3) strong and homogeneous enhancement on arterial phase CEUS, CT or MR with a central vascular supply, which becomes similar to adjacent liver on portal and delayed phases, 4) central scar best seen on MRI (hypointense on pre-contrast T1-weighted images, strongly hyperintense on T2-weighted images, and becoming hyperintense on delayed phase using extracellular MR contrast agents because of the ac-

cumulation of contrast material in the fibrous tissue), and 5) lack of capsule with often lobulated contours [65].

Generally, the diagnosis of FNH is based on the combination of several imaging modalities, whereby the MRI and CEUS has the highest sensitivity, especially for lesions >3 cm [3,4,112-115]. Compared to US and CT, the MRI has the highest sensitivity, although according to Soussan et al it is strongly dependent on the examiner (63-88%). On the other hand, the specificity of the MRI for FNH diagnostics is with almost 100% very high. However, especially for small FNH without central scar, MRI diagnosis is difficult. For FNH <3 cm CEUS is recommended [65,112,116].

Ultrasound

The FNH is usually an incidental finding [64,117-120]. It often presents isoechogenic or discreetly hypoechogenic to the surrounding liver tissue and is therefore often not clearly visible in the B-mode. In the fatty liver, the FNH can also appear considerably hypoechogenic [7,121,122]. Occasionally, the typical spoke-wheel sign (SWS), which is caused by the central feeding artery with radially spreading septa, can sometimes already be seen in the B-mode. Typically, the FNH shows no signs of infiltration, but it can compress nearby vessels [52,60]. In native colour or power mode US, the central artery can often be seen with increased blood flow compared to the surrounding liver tissue [52,123]. Therefore, Doppler US can be used to detect the flow signal in the feeding artery and determine the resistive index [6,124,125] (fig 5).

CEUS

In CEUS, FNH typically shows early arterial phase hyperenhancement (APHE) compared to surrounding liver tissue [126-130]. Between 10-20 seconds after injection of the contrast agent, the specific radial vascular pattern (SWS) appears [110,131]. This is followed by a centrifugal uptake of the contrast agent so that the whole lesion appears hyperechogenic within seconds. This fast dynamic process can be missed by CT or MRI. In the

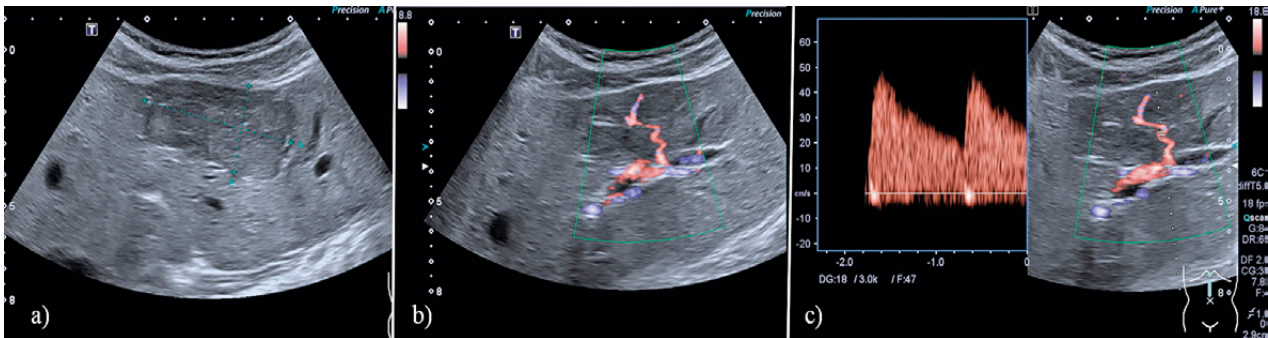


Fig 5. Flow signal of a feeding artery. B-mode ultrasound (a), color Doppler ultrasound (b) and spectral Doppler ultrasound showing a central feeding artery in FNH with low resistance profile (c) [6,124,125].

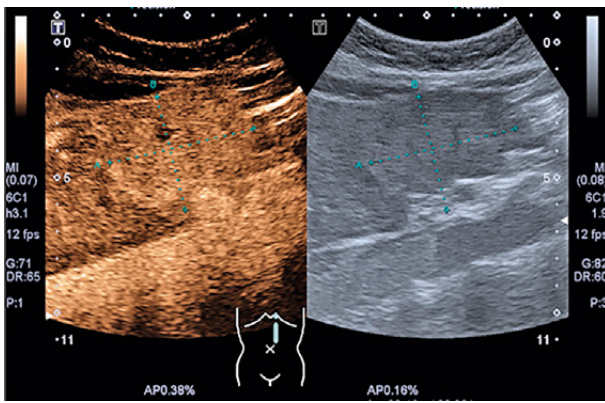


Fig 6. Central scar without contrast enhancement. CEUS with late venous phase with typical “scar star” due to dystrophic central artery.

portal venous phase, the contrast in FNH appears hyper-enhancing (95 %) or at least iso-enhancing compared to the surrounding liver [104,132]. In the late venous phase in typical FNH the central scar can be demonstrated with loss of contrast agent in up to 70% of patients (fig 6). CEUS represents the ideal diagnostic tool for FNH < 3 cm [65,97,112,116].

Superb Micro-Vascular Imaging

SMI appears to be an interesting diagnostic tool for the visualisation of microvascular structures of FNH since FNH is characterized by typical macro- and micro-vascular patterns. Since the SMI is still a new tool, there is still a small number of publications about this topic.

For the first time SMI was described as an option for the diagnosis of FNH 2016 by Lee et al in a case series of 29 liver lesions including 7 FNH, with a diameter of 8 mm to 28 mm. The typical SWS could be demonstrated in 3/7 cases with SMI, in 2/7 cases a radiating pattern could be seen and in 2 cases the signal was not specific. The size of the lesions for which the SMI signal was un-specific was unfortunately not mentioned [133]. Also, in 2016 Bonacchi et al described the diagnosis of FNH using SMI in two cases (diameter 30 mm and 15 mm) [62]. A prospective study by He et al followed in 2017, in which a total of 31 different liver lesions (FNH n=2) were analyzed. The typical SWS could be demonstrated in both FNH (4 cm) [58]. In 2017 Naganuma et al described another two cases of 70 mm and 50 mm FNH diagnosed with SMI [61]. In the first European experience on SMI and FNH, a case series (n=5) has shown

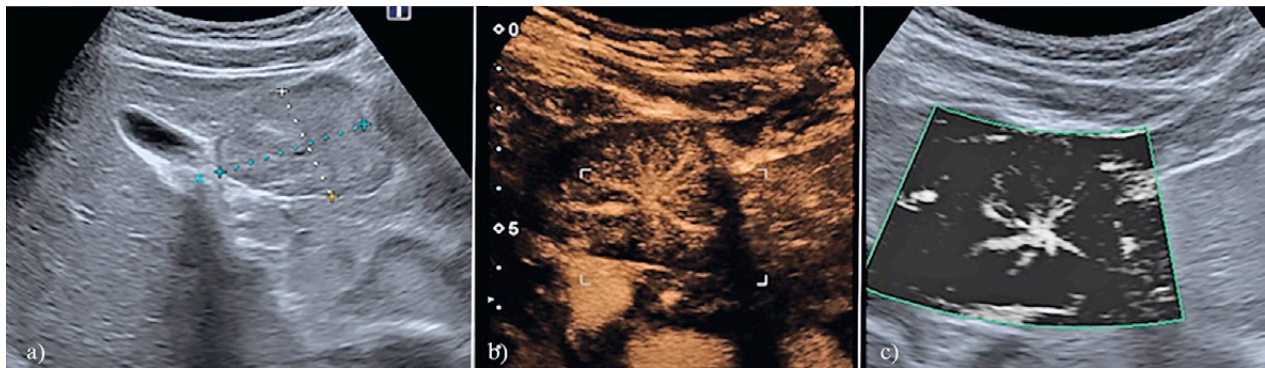


Fig 7. A 55-year-old asymptomatic woman with incidental focal liver lesion of 4 cm FNH on conventional ultrasound (a). CEUS with arterial spoke-wheel sign (b). SMI with typical spoke-wheel pattern (c).

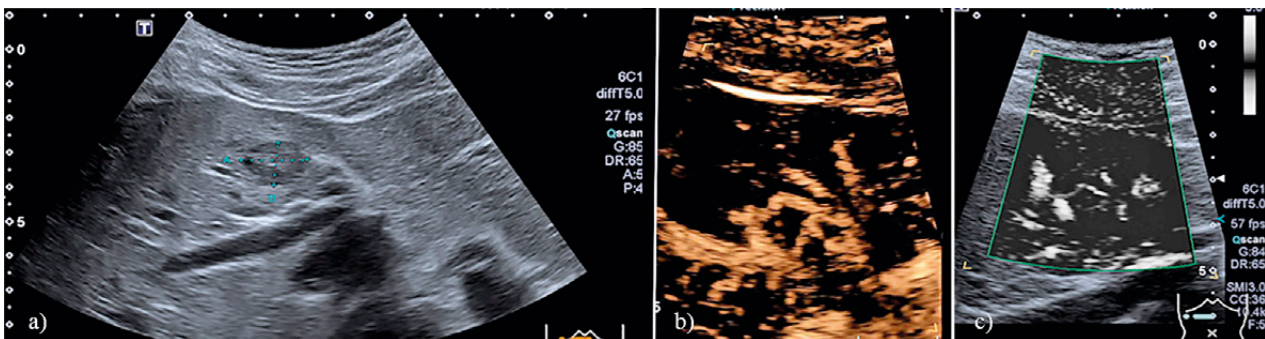


Fig 8. A 25-year-old woman who presented with suspected autoimmune pancreatitis. Pancreas-MRI incidentally showed an FLL of 1.8 cm of unclear dignity. SOR was CEUS with a of 18-month follow-up. B-mode Ultrasound showing 1.8 cm FNH (a), CEUS with arterial spoke-wheel enhancement(b) and SMI with spoke-wheel pattern (c).

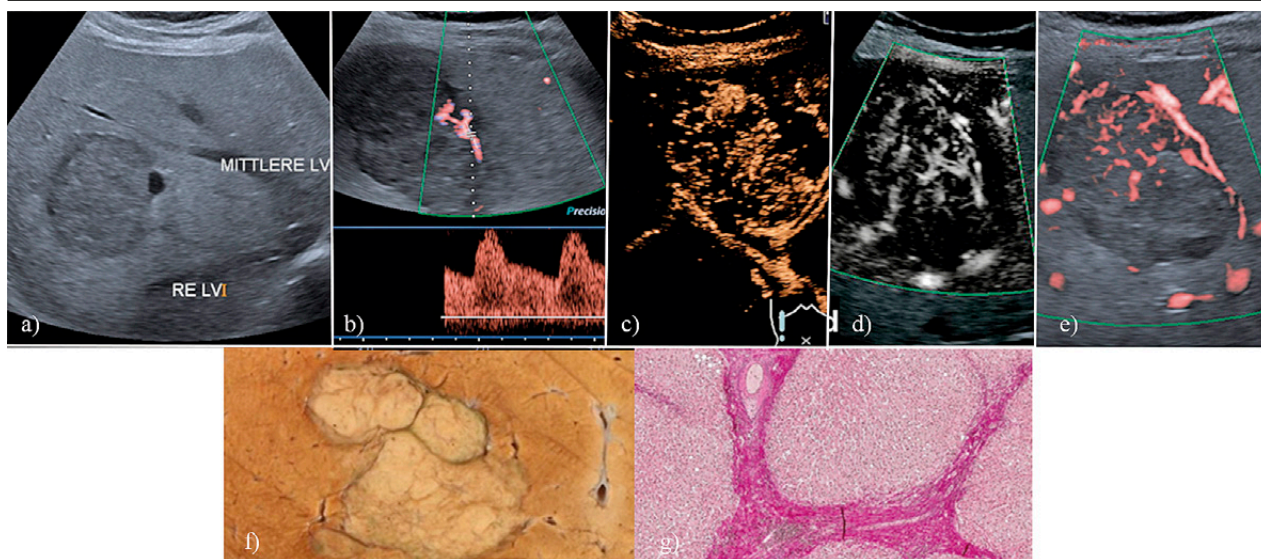


Fig 9. A 24 year-old women with pain in the upper right abdomen with an FLL, doubling in size from 3 cm to 6 cm within 2 years in liver segment VIII (a). Flow signal of a feeding artery with Doppler ultrasound showing a eccentric feeding artery in FNH with low resistance profile (b), CEUS with teleangiectatic “atypical” FNH (Type III) (c), monochrome SMI (d), color SMI (e). Resected FNH (f). Histopathological analysis demonstrated fibrous and thickened walls of the blood vessels (Elastica-van-Gieson-stain) (g).

a reliable representation of the SWS in SMI mode [134]. The lesions ranged from 18 mm to 60 mm diameter.

Principally, the device settings on the US machine are based on the general recommendations shown above. A more detailed description of the settings can be found in the reports by Lee et al and He et al. Both groups used the following settings: convex probe (1-6 MHz), color velocity scale ≤ 2.0 cm/s, frame rate >30 fps, color frequency 5-7 MHz, and the gain setting adjusted to show optimal imaging [58,60].

In our experience, the ROI should be as small as possible but finally adapted to the size of the FNH. Principally we first use the conventional Doppler and then the more specific modes (first cSMI and then the mSMI mode) to get an overview of the lesion and to adjust the ROI. Finally, a fine adjustment is made with the time smoothing function (frame averaging) starting using the scale “1” and scaling upwards until the optimal vascular visualization is reached. For documentation purposes, the patient is asked for breath holding, what further improves the image despite the propagated automatic correction of motion artifacts (fig 7-9).

Conclusion

With the introduction of SMI, the spectrum of ultrasound has been extended by another promising non-invasive diagnostic imaging tool to visualize small vessels with slow blood flows in real time and without intravenous contrast agents. The analysis of contrast en-

hancement using time intensity curve analysis cannot be replaced [5,135,136], which are important to differentiate malignant and benign FLL [3,4]. In conclusion, SMI rather represents an additive tool than a substitute for CEUS or MRI.

Conflict of interest: none

Acknowledgment: We would like to thank Dr. Jörg Neuweiler for the photos of the histological specimens, Canon Medical Systems AG, (formerly Toshiba) for the permission to use the figures explaining the SMI filter functions, Dr. Rahel Häuptle for the SMI images of her charming kidney cortex.

References

1. Dietrich CF, Bolondi L, Duck F, et al. History of Ultrasound in Medicine from its birth to date (2022), on occasion of the 50 Years Anniversary of EFSUMB. A publication of the European Federation of Societies for Ultrasound In Medicine and Biology (EFSUMB), designed to record the historical development of medical ultrasound. *Med Ultrason* 2022;24:434-450.
2. Merz E, Evans DH, Dong Y, Jenssen C, Dietrich CF. History of ultrasound in obstetrics and gynaecology from 1971 to 2021 on occasion of the 50 years anniversary of EFSUMB. *Med Ultrason* 2023;25:175-188.
3. Dietrich CF, Nolsoe CP, Barr RG, et al. Guidelines and Good Clinical Practice Recommendations for Contrast-Enhanced Ultrasound (CEUS) in the Liver-Update 2020 WFUMB in Cooperation with EFSUMB, AFSUMB,

- AIUM, and FLAUS. *Ultrasound Med Biol* 2020;46:2579-2604.
4. Dietrich CF, Nolsoe CP, Barr RG, et al. Guidelines and Good Clinical Practice Recommendations for Contrast Enhanced Ultrasound (CEUS) in the Liver - Update 2020 - WFUMB in Cooperation with EFSUMB, AFSUMB, AIUM, and FLAUS. *Ultraschall Med* 2020;41:562-585.
 5. Dietrich CF, Averkiou M, Nielsen MB, et al. How to perform Contrast-Enhanced Ultrasound (CEUS). *Ultrasound Int Open* 2018;4:E2-E15.
 6. Dong Y, Wang WP, Ignee A, et al. The Diagnostic Value of Doppler Resistive Index in the differential diagnosis of focal liver lesions. *J Ultrason* 2023;23(93):e45-e52.
 7. Dietrich CF, Shi L, Lowe A, et al. Conventional ultrasound for diagnosis of hepatic steatosis is better than believed. *Z Gastroenterol* 2022;60:1235-1248.
 8. Lowe A, Jenssen C, Huske S, et al. "Knobology" in Doppler Ultrasound. *Med Ultrason* 2021;23:480-486.
 9. Seitz K, Strobel D. A Milestone: Approval of CEUS for Diagnostic Liver Imaging in Adults and Children in the USA. *Ultraschall Med* 2016;37:229-232.
 10. Dietrich CF, Kratzer W, Strobe D, et al. Assessment of metastatic liver disease in patients with primary extrahepatic tumors by contrast-enhanced sonography versus CT and MRI. *World J.Gastroenterol* 2006;12:1699-1705.
 11. Ignee A, Moeller K, Thees-Laurenz R, et al. Comments and illustrations of the WFUMB CEUS liver guidelines: Rare focal liver lesions - infectious, bacterial. *Med Ultrason* 2023;25:312-324
 12. Moeller K, Stock B, Ignee A, et al. Comments and illustrations of the WFUMB CEUS liver guidelines. Rare focal liver lesion – non infectious, non-neoplastic. *Med Ultrason* 2023, doi: 10.11152/mu-4192.
 13. Zander T, Safai Zadeh E, Moeller K, et al. Comments and illustrations of the WFUMB CEUS liver guidelines: Infectious FLL parasitic and fungi. *Med Ultrason* 2023, doi: 10.11152/mu-4091.
 14. Moller K, Tscheu T, De Molo C, et al. Comments and illustrations of the WFUMB CEUS liver guidelines: rare congenital vascular pathology. *Med Ultrason* 2022;24:461-472.
 15. Park AY, Seo BK. Up-to-date Doppler techniques for breast tumor vascularity: superb microvascular imaging and contrast-enhanced ultrasound. *Ultrasonography* 2018;37:98-106.
 16. Hata J. Seeing the Unseen New Techniques in Vascular Imaging. *Medicine* 2014.
 17. Sharma M, Hollerbach S, Fusaroli P, et al. General principles of image optimization in EUS. *Endosc Ultrasound* 2021;10:168-184.
 18. Zander D, Huske S, Hoffmann B, et al. Ultrasound Image Optimization ("Knobology"): B-Mode. *Ultrasound Int Open* 2020;6:E14-E24.
 19. Jenssen C, Tuma J, Moller K, et al. [Ultrasound artifacts and their diagnostic significance in internal medicine and gastroenterology - part 2: color and spectral Doppler artifacts]. *Z Gastroenterol* 2016;54:569-578.
 20. Tuma J, Jenssen C, Moller K, et al. [Ultrasound artifacts and their diagnostic significance in internal medicine and gastroenterology - Part 1: B-mode artifacts]. *Z Gastroenterol* 2016;54:433-450.
 21. Kruskal JB, Newman PA, Sammons LG, Kane RA. Optimizing Doppler and color flow US: application to hepatic sonography. *Radiographics* 2004;24:657-675.
 22. Jenssen C, Lorentzen T, Dietrich CF, et al. Incidental Findings of Gallbladder and Bile Ducts-Management Strategies: General Aspects, Gallbladder Polyps and Gallbladder Wall Thickening-A World Federation of Ultrasound in Medicine and Biology (WFUMB) Position Paper. *Ultrasound Med Biol* 2022;48:2355-2378.
 23. Dietrich CF, Braden B, Burmeister S, et al. How to perform EUS-guided biliary drainage. *Endosc Ultrasound* 2022;11:342-354.
 24. Hocke M, Burmeister S, Braden B, et al. Controversies in EUS-guided treatment of walled-off necrosis. *Endosc Ultrasound* 2022;11:442-457.
 25. Moller K, Braden B, Culver EL, et al. Secondary sclerosing cholangitis and IgG4-sclerosing cholangitis - A review of cholangiographic and ultrasound imaging. *Endosc Ultrasound* 2023;12:181-199.
 26. Park AY, Seo BK, Cha SH, Yeom SK, Lee SW, Chung HH. An Innovative Ultrasound Technique for Evaluation of Tumor Vascularity in Breast Cancers: Superb Micro-Vascular Imaging. *J Breast Cancer* 2016;19:210-213.
 27. Yongfeng Z, Ping Z, Wengang L, Yang S, Shuangming T. Application of a Novel Microvascular Imaging Technique in Breast Lesion Evaluation. *Ultrasound Med Biol* 2016;42:2097-2105.
 28. Zhu YC, Zhang Y, Deng SH, Jiang Q. Diagnostic Performance of Superb Microvascular Imaging (SMI) Combined with Shear-Wave Elastography in Evaluating Breast Lesions. *Med Sci Monit* 2018;24:5935-5942.
 29. Bakdik S, Arslan S, Oncu F, et al. Effectiveness of Superb Microvascular Imaging for the differentiation of intraductal breast lesions. *Med Ultrason* 2018;20:306-312.
 30. Zhu YC, Zhang Y, Deng SH, Jiang Q, Shi XR, Feng LL. Evaluation of plasma cell mastitis with superb microvascular imaging. *Clin Hemorheol Microcirc* 2019;72:129-138.
 31. Kim ES, Seo BK, Park EK, et al. Significance of microvascular evaluation of ductal lesions on breast ultrasonography: Influence on diagnostic performance. *Clin Imaging* 2018;51:252-259.
 32. Xiao XY, Chen X, Guan XF, Wu H, Qin W, Luo BM. Superb microvascular imaging in diagnosis of breast lesions: a comparative study with contrast-enhanced ultrasonographic microvascular imaging. *Br J Radiol* 2016;89:20160546.
 33. Zhan J, Diao XH, Jin JM, Chen L, Chen Y. Superb Microvascular Imaging-A new vascular detecting ultrasonographic technique for avascular breast masses: A preliminary study. *Eur J Radiol* 2016;85:915-921.
 34. Ma Y, Li G, Li J, Ren WD. The Diagnostic Value of Superb Microvascular Imaging (SMI) in Detecting Blood Flow Signals of Breast Lesions: A Preliminary Study Comparing

- SMI to Color Doppler Flow Imaging. *Medicine (Baltimore)* 2015;94:e1502.
35. Park AY, Seo BK, Woo OH, et al. The utility of ultrasound superb microvascular imaging for evaluation of breast tumour vascularity: comparison with colour and power Doppler imaging regarding diagnostic performance. *Clin Radiol* 2018;73:304-311.
 36. Li YH, Wen DH, Li CX, Li XJ, Xue G. [The role of ATA (2015) guidelines, superb microvascular imaging, and spectral Doppler in differentiation between malignant and benign thyroid nodules]. *Lin Chung Er Bi Yan Hou Tou Jing Wai Ke Za Zhi* 2017;31:1152-1156.
 37. Machado P, Segal S, Lyshchik A, Forsberg F. A Novel Microvascular Flow Technique: Initial Results in Thyroids. *Ultrasound Q* 2016;32:67-74.
 38. Zhu YC, Zhang Y, Deng SH, Jiang Q. A Prospective Study to Compare Superb Microvascular Imaging with Grayscale Ultrasound and Color Doppler Flow Imaging of Vascular Distribution and Morphology in Thyroid Nodules. *Med Sci Monit* 2018;24:9223-9231.
 39. Yoon JH, Kim EK, Kwak JY, Park VY, Moon HJ. Application of Various Additional Imaging Techniques for Thyroid Ultrasound: Direct Comparison of Combined Various Elastography and Doppler Parameters to Gray-Scale Ultrasound in Differential Diagnosis of Thyroid Nodules. *Ultrasound Med Biol* 2018;44:1679-1686.
 40. Bayramoglu Z, Kandemirli SG, Caliskan E, et al. Assessment of paediatric Hashimoto's thyroiditis using superb microvascular imaging. *Clin Radiol* 2018;73:1059 e1059-1059 e1015.
 41. Ahn HS, Lee JB, Seo M, Park SH, Choi BI. Distinguishing benign from malignant thyroid nodules using thyroid ultrasonography: utility of adding superb microvascular imaging and elastography. *Radiol Med* 2018;123:260-270.
 42. Kong J, Li JC, Wang HY, et al. Role of Superb Micro-Vascular Imaging in the Preoperative Evaluation of Thyroid Nodules: Comparison With Power Doppler Flow Imaging. *J Ultrasound Med* 2017;36:1329-1337.
 43. Lu R, Meng Y, Zhang Y, et al. Superb microvascular imaging (SMI) compared with conventional ultrasound for evaluating thyroid nodules. *BMC Med Imaging* 2017;17:65.
 44. Zhu YC, Jiang XZ, Bai QK, et al. Evaluating the Efficacy of Atorvastatin on Patients with Carotid Plaque by an Innovative Ultrasonography. *J Stroke Cerebrovasc Dis* 2019;28:830-837.
 45. Xie X, Bai ZY, Liu Y, Zhang HB. [Value of Superb Microvascular Imaging in Diagnosing Carotid Artery Vulnerable Plaque]. *Zhongguo Yi Xue Ke Xue Yuan Xue Bao* 2018;40:444-449.
 46. Cantisani V, David E, Ferrari D, et al. Color Doppler Ultrasound with Superb Microvascular Imaging Compared to Contrast-enhanced Ultrasound and Computed Tomography Angiography to Identify and Classify Endoleaks in Patients Undergoing EVAR. *Ann Vasc Surg* 2017;40:136-145.
 47. Oura K, Kato T, Ohba H, Terayama Y. Evaluation of Intraplaque Neovascularization Using Superb Microvascular Imaging and Contrast-Enhanced Ultrasonography. *J Stroke Cerebrovasc Dis* 2018;27:2348-2353.
 48. Gabriel M, Tomczak J, Snoch-Ziolkiewicz M, et al. Superb Micro-vascular Imaging (SMI): a Doppler ultrasound technique with potential to identify, classify, and follow up endoleaks in patients after Endovascular Aneurysm Repair (EVAR). *Abdom Radiol (NY)* 2018;43:3479-3486.
 49. Guven F, Karaca L, Ogul H, Sade R, Ozturk G, Kantarci M. The Value of Superb Microvascular Imaging in Detecting Hepatic Artery Occlusion in Liver Transplantation: A Preliminary Study. *Ultrasound Q* 2019;35:325-329.
 50. Hoshino M, Shimizu T, Ogura H, et al. Intraplaque Microvascular Flow Signal in Superb Microvascular Imaging and Magnetic Resonance Imaging Carotid Plaque Imaging in Patients with Atheromatous Carotid Artery Stenosis. *J Stroke Cerebrovasc Dis* 2018;27:3529-3534.
 51. Jang HY, Kim KW, Kim SY, et al. Visibility of the graft hepatic artery using superb microvascular imaging in liver transplantation recipients: initial experience. *Acta Radiol* 2018;59:1326-1335.
 52. Becker D, Becker HD, Bernatik T, et al. Klinische Sonographie und sonographische Differenzialdiagnose. In: Seitz K, Schuler A, Rettenmaier G, editors. 2., komplett neu bearbeitete und erweiterte Auflage ed. Stuttgart: Georg Thieme Verlag KG; 2008.
 53. Orlandi D, Gitto S, Perugin Bernardi S, et al. Advanced Power Doppler Technique Increases Synovial Vascularity Detection in Patients with Rheumatoid Arthritis. *Ultrasound Med Biol* 2017;43:1880-1887.
 54. Yokota K, Tsuzuki Wada T, Akiyama Y, Mimura T. Detection of synovial inflammation in rheumatic diseases using superb microvascular imaging: Comparison with conventional power Doppler imaging. *Mod Rheumatol* 2018;28:327-333.
 55. Lim AKP, Satchithananda K, Dick EA, Abraham S, Cosgrove DO. Microflow imaging: New Doppler technology to detect low-grade inflammation in patients with arthritis. *Eur Radiol* 2018;28:1046-1053.
 56. Yu X, Li Z, Ren M, Xi J, Wu J, Ji Y. Superb microvascular imaging (SMI) for evaluating hand joint lesions in patients with rheumatoid arthritis in clinical remission. *Rheumatol Int* 2018;38:1885-1890.
 57. Arslan S, Karahan AY, Oncu F, Bakdik S, Durmaz MS, Tolu I. Diagnostic Performance of Superb Microvascular Imaging and Other Sonographic Modalities in the Assessment of Lateral Epicondylitis. *J Ultrasound Med* 2018;37:585-593.
 58. He MN, Lv K, Jiang YX, Jiang TA. Application of superb microvascular imaging in focal liver lesions. *World J Gastroenterol* 2017;23:7765-7775.
 59. Dubinsky TJ, Revels J, Wang S, et al. Comparison of Superb Microvascular Imaging With Color Flow and Power Doppler Imaging of Small Hepatocellular Carcinomas. *J Ultrasound Med* 2018;37:2915-2924.
 60. Lee DH, Lee JY, Han JK. Superb microvascular imaging technology for ultrasound examinations: Initial experiences for hepatic tumors. *Eur J Radiol* 2016;85:2090-2095.

61. Naganuma H, Ishida H, Ogawa M, Suzuki K. Visualization of draining vein in focal nodular hyperplasia by superb microvascular imaging: report of two cases. *J Med Ultrason* (2001) 2017;44:323-328.
62. Bonacchi G, Becciolini M, Seghieri M. Superb microvascular imaging: a potential tool in the detection of FNH. *J Ultrasound* 2017;20:179-180.
63. Moller K, Safai Zadeh E, Gorg C, et al. Prevalence of benign focal liver lesions and non-hepatocellular carcinoma malignant lesions in liver cirrhosis. *Z Gastroenterol* 2022.
64. Dietrich CF, Fraser AG, Dong Y, et al. Managing Incidental Findings Reported by Medical, Sonography and Other Students Performing Educational Ultrasound Examinations. *Ultrasound Med Biol* 2022;48:180-187.
65. European Association for the Study of the L. EASL Clinical Practice Guidelines on the management of benign liver tumours. *J Hepatol* 2016;65:386-398.
66. Marrero JA, Ahn J, Rajender Reddy K, Americal College of G. ACG clinical guideline: the diagnosis and management of focal liver lesions. *Am J Gastroenterol* 2014;109:1328-1347; quiz 1348.
67. Rubin RA, Mitchell DG. Evaluation of the solid hepatic mass. *Med Clin North Am* 1996;80:907-928.
68. Wanless IR, Mawdsley C, Adams R. On the pathogenesis of focal nodular hyperplasia of the liver. *Hepatology* 1985;5:1194-1200.
69. Nahm CB, Ng K, Lockie P, Samra JS, Hugh TJ. Focal nodular hyperplasia—a review of myths and truths. *J Gastrointest Surg* 2011;15:2275-2283.
70. Nguyen BN, Flejou JF, Terris B, Belghiti J, Degott C. Focal nodular hyperplasia of the liver: a comprehensive pathologic study of 305 lesions and recognition of new histologic forms. *Am J Surg Pathol* 1999;23:1441-1454.
71. Ji Y, Chen S, Xiang B, et al. Clinical Features of Focal Nodular Hyperplasia of the Liver in Children. *J Pediatr Gastroenterol Nutr* 2016;62:813-818.
72. Stocker JT, Ishak KG. Focal nodular hyperplasia of the liver: a study of 21 pediatric cases. *Cancer* 1981;48:336-345.
73. Ferraioli G, Barr RG, Farrokh A, et al. How to perform shear wave elastography. Part I. *Med Ultrason* 2022;24:95-106.
74. Ferraioli G, Barr RG, Farrokh A, et al. How to perform shear wave elastography. Part II. *Med Ultrason* 2022;24:196-210.
75. Dietrich CF, Augustiniene R, Batko T, et al. European Federation of Societies for Ultrasound in Medicine and Biology (EFSUMB): An Update on the Pediatric CEUS Registry on Behalf of the “EFSUMB Pediatric CEUS Registry Working Group”. *Ultraschall Med* 2021;42:270-277.
76. Dietrich CF, Ferraioli G, Sirlin R, et al. General advice in ultrasound based elastography of pediatric patients. *Med Ultrason* 2019;21:315-326.
77. Sidhu PS, Cantisani V, Deganello A, et al. Role of Contrast-Enhanced Ultrasound (CEUS) in Paediatric Practice: An EFSUMB Position Statement. *Ultraschall Med* 2017;38:33-43.
78. Dong Y, Koch J, Alhyari A, et al. Ultrasound Elastography for Characterization of Focal Liver Lesions. *Z Gastroenterol* 2022.
79. Bouyn CI, Leclere J, Raimondo G, et al. Hepatic focal nodular hyperplasia in children previously treated for a solid tumor. Incidence, risk factors, and outcome. *Cancer* 2003;97:3107-3113.
80. Dietrich CF, Mertens JC, Braden B, Schuessler G, Ott M, Ignee A. Contrast-enhanced ultrasound of histologically proven liver hemangiomas. *Hepatology* 2007;45:1139-1145.
81. Leoni FG, Magnano San Lio P, De Molo C, et al. Budd-Chiari syndrome (BCS): a challenging diagnosis not to be overlooked—single center report and pictorial essay. *J Ultrasound* 2022.
82. Wiest I, Teufel A, Ebert MP, et al. [Budd-Chiari syndrome, review and illustration]. *Z Gastroenterol* 2022;60:1335-1345.
83. Ignee A, Weiper D, Schuessler G, Teuber G, Faust D, Dietrich CF. Sonographic characterisation of hepatocellular carcinoma at time of diagnosis. *Z.Gastroenterol*. 2005;43:289-294.
84. Dietrich CF, Trenker C, Fontanilla T, et al. New Ultrasound Techniques Challenge the Diagnosis of Sinusoidal Obstruction Syndrome. *Ultrasound Med Biol* 2018;44:2171-2182.
85. Trenker C, Sohlbach K, Dietrich CF, Gorg C. Clinical diagnosis of veno-occlusive disease using contrast enhanced ultrasound. *Bone Marrow Transplant* 2018;53:1369-1371.
86. Kirchner J, Zipf A, Dietrich CF, Hohmann A, Heyd R, Berkefeld J. [Universal organ involvement in Rendu-Osler-Weber disease: interdisciplinary diagnosis and interventional therapy]. *Z.Gastroenterol*. 1996;34:747-752.
87. Brancatelli G, Federle MP, Grazioli L, Blachar A, Peterson MS, Thaete L. Focal nodular hyperplasia: CT findings with emphasis on multiphasic helical CT in 78 patients. *Radiology* 2001;219:61-68.
88. Vilgrain V, Uzan F, Brancatelli G, Federle MP, Zappa M, Menu Y. Prevalence of hepatic hemangioma in patients with focal nodular hyperplasia: MR imaging analysis. *Radiology* 2003;229:75-79.
89. D’Halluin V, Vilgrain V, Pelletier G, et al. [Natural history of focal nodular hyperplasia. A retrospective study of 44 cases]. *Gastroenterol Clin Biol* 2001;25:1008-1010.
90. Ramirez-Fuentes C, Marti-Bonmati L, Torregrosa A, Del Val A, Martinez C. Variations in the size of focal nodular hyperplasia on magnetic resonance imaging. *Radiologia* 2013;55:499-504.
91. Rifai K, Mix H, Krusche S, Potthoff A, Manns MP, Gebel MJ. No evidence of substantial growth progression or complications of large focal nodular hyperplasia during pregnancy. *Scand J Gastroenterol* 2013;48:88-92.
92. Dietrich CF, Tannapfel A, Jang HJ, Kim TK, Burns PN, Dong Y. Ultrasound Imaging of Hepatocellular Adenoma Using the New Histology Classification. *Ultrasound Med Biol* 2019;45:1-10.
93. Dietrich CF, Tana C, Caraianni C, Dong Y. Contrast enhanced ultrasound (CEUS) imaging of solid benign focal liver lesions. *Expert Rev Gastroenterol Hepatol* 2018;12:479-489.
94. Dong Y, Wang WP, Mao F, et al. Contrast enhanced ultrasound features of hepatic cystadenoma and hepatic cystadenocarcinoma. *Scand J Gastroenterol* 2017;52:365-372.

95. Chiorean L, Cui XW, Tannapfel A, et al. Benign liver tumors in pediatric patients - Review with emphasis on imaging features. *World J Gastroenterol* 2015;21:8541-8561.
96. Perrakis A, Demir R, Muller V, et al. Management of the focal nodular hyperplasia of the liver: evaluation of the surgical treatment comparing with observation only. *Am J Surg* 2012;204:689-696.
97. Dietrich CF, Schuessler G, Trojan J, Fellbaum C, Ignee A. Differentiation of focal nodular hyperplasia and hepatocellular adenoma by contrast-enhanced ultrasound. *Br.J.Radiol.* 2005;78:704-707.
98. Maillette de Buy Wenniger L, Terpstra V, Beuers U. Focal nodular hyperplasia and hepatic adenoma: epidemiology and pathology. *Dig Surg* 2010;27:24-31.
99. Weimann A, Ringe B, Klempnauer J, et al. Benign liver tumors: differential diagnosis and indications for surgery. *World J Surg* 1997;21:983-990; discussion 990-981.
100. Colli A, Fraquelli M, Massironi S, Colucci A, Paggi S, Conte D. Elective surgery for benign liver tumours. *Cochrane Database Syst Rev* 2007;2007:CD005164.
101. Amesur N, Hammond JS, Zajko AB, Geller DA, Gamblin TC. Management of unresectable symptomatic focal nodular hyperplasia with arterial embolization. *J Vasc Interv Radiol* 2009;20:543-547.
102. Hedayati P, VanSonnenberg E, Shamos R, Gillespie T, McMullen W. Treatment of symptomatic focal nodular hyperplasia with percutaneous radiofrequency ablation. *J Vasc Interv Radiol* 2010;21:582-585.
103. Buscarini E, Danesino C, Plauchu H, et al. High prevalence of hepatic focal nodular hyperplasia in subjects with hereditary hemorrhagic telangiectasia. *Ultrasound Med Biol* 2004;30:1089-1097.
104. Dietrich CF, Maddalena ME, Cui XW, Schreiber-Dietrich D, Ignee A. Liver tumor characterization--review of the literature. *Ultraschall Med* 2012;33 Suppl 1:S3-10.
105. Dong Y, Wang WP, Mao F, et al. Imaging Features of Fibrolamellar Hepatocellular Carcinoma with Contrast-Enhanced Ultrasound. *Ultraschall Med* 2020.
106. Dong Y, Wang WP, Lim A, et al. Ultrasound findings in peliosis hepatis. *Ultrasonography* 2021;40:546-554.
107. Zarzour JG, Porter KK, Tchepeli H, Robbin ML. Contrast-enhanced ultrasound of benign liver lesions. *Abdom Radiol (NY)* 2018;43:848-860.
108. Rebouissou S, Bioulac-Sage P, Zucman-Rossi J. Molecular pathogenesis of focal nodular hyperplasia and hepatocellular adenoma. *J Hepatol* 2008;48:163-170.
109. Rebouissou S, Couchy G, Libbrecht L, et al. The beta-catenin pathway is activated in focal nodular hyperplasia but not in cirrhotic FNH-like nodules. *J Hepatol* 2008;49:61-71.
110. Grazioli L, Morana G, Kirchin MA, Schneider G. Accurate differentiation of focal nodular hyperplasia from hepatic adenoma at gadobenate dimeglumine-enhanced MR imaging: prospective study. *Radiology* 2005;236:166-177.
111. Bioulac-Sage P, Laumonier H, Rullier A, et al. Over-expression of glutamine synthetase in focal nodular hyperplasia: a novel easy diagnostic tool in surgical pathology. *Liver Int* 2009;29:459-465.
112. Soussan M, Aube C, Bahrami S, Boursier J, Valla DC, Vilgrain V. Incidental focal solid liver lesions: diagnostic performance of contrast-enhanced ultrasound and MR imaging. *Eur Radiol* 2010;20:1715-1725.
113. Claudon M, Dietrich CF, Choi BI, et al. Guidelines and good clinical practice recommendations for Contrast Enhanced Ultrasound (CEUS) in the liver - update 2012: A WFUMB-EFSUMB initiative in cooperation with representatives of AFSUMB, AIUM, ASUM, FLAUS and ICUS. *Ultrasound Med Biol* 2013;39:187-210.
114. Claudon M, Dietrich CF, Choi BI, et al. Guidelines and good clinical practice recommendations for contrast enhanced ultrasound (CEUS) in the liver--update 2012: a WFUMB-EFSUMB initiative in cooperation with representatives of AFSUMB, AIUM, ASUM, FLAUS and ICUS. *Ultraschall Med* 2013;34:11-29.
115. Claudon M, Cosgrove D, Albrecht T, et al. Guidelines and good clinical practice recommendations for contrast enhanced ultrasound (CEUS) - update 2008. *Ultraschall Med* 2008;29:28-44.
116. Leen E, Ceccotti P, Kalogeropoulou C, Angerson WJ, Moug SJ, Horgan PG. Prospective multicenter trial evaluating a novel method of characterizing focal liver lesions using contrast-enhanced sonography. *AJR Am J Roentgenol* 2006;186:1551-1559.
117. Trenker C, Gorg C, Freeman S, et al. WFUMB Position Paper-Incidental Findings, How to Manage: Spleen. *Ultrasound Med Biol* 2021;47:2017-2032.
118. Chiorean L, Cantisani V, Jenssen C, Sidhu PS, Baum U, Dietrich CF. Focal masses in a non-cirrhotic liver: The additional benefit of CEUS over baseline imaging. *Eur J Radiol* 2015;84:1636-1643.
119. Dietrich CF, Sharma M, Gibson RN, Schreiber-Dietrich D, Jenssen C. Fortuitously discovered liver lesions. *World J Gastroenterol* 2013;19:3173-3188.
120. Dietrich CF, Jenssen C. [Focal liver lesion, incidental finding]. *Dtsch Med Wochenschr* 2012;137:2099-2116.
121. Ferraioli G, Berzigotti A, Barr RG, et al. Quantification of Liver Fat Content with Ultrasound: A WFUMB Position Paper. *Ultrasound Med Biol* 2021;47:2803-2820.
122. Hirche TO, Ignee A, Hirche H, Schneider A, Dietrich CF. Evaluation of hepatic steatosis by ultrasound in patients with chronic hepatitis C virus infection. *Liver Int.* 2007;27:748-757.
123. Bartolozzi C, Lencioni R, Paolicchi A, Moretti M, Armilotta N, Pinto F. Differentiation of hepatocellular adenoma and focal nodular hyperplasia of the liver: comparison of power Doppler imaging and conventional color Doppler sonography. *Eur Radiol* 1997;7:1410-1415.
124. Tana C, Schiavone C, Ticinesi A, et al. Hepatic artery resistive index as surrogate marker for fibrosis progression in NAFLD patients: A clinical perspective. *Int J Immunopathol Pharmacol* 2018;32:2058738418781373.

125. Ignee A, Boerner N, Bruening A, et al. Duplexsonography of the mesenteric vessels - a critical evaluation of inter observer variability. *Z Gastroenterol* 2016;54:304-311.
126. Schellhaas B, Bernatik T, Bohle W, et al. Contrast-Enhanced Ultrasound Algorithms (CEUS-LIRADS/ESCU-LAP) for the Noninvasive Diagnosis of Hepatocellular Carcinoma - A Prospective Multicenter DEGUM Study. *Ultraschall Med* 2021;42:178-186.
127. Caraiani C, Boca B, Bura V, Sparchez Z, Dong Y, Dietrich C. CT/MRI LI-RADS v2018 vs. CEUS LI-RADS v2017- Can Things Be Put Together? *Biology (Basel)* 2021;10.
128. Dietrich CF, Dong Y, Kono Y, et al. LI-RADS ancillary features on contrast-enhanced ultrasonography. *Ultrasonography* 2020;39:221-228.
129. Li J, Chen M, Wang ZJ, et al. Interobserver agreement for contrast-enhanced ultrasound of liver imaging reporting and data system: A systematic review and meta-analysis. *World J Clin Cases* 2020;8:5589-5602.
130. Wang JY, Feng SY, Xu JW, et al. Usefulness of the Contrast-Enhanced Ultrasound Liver Imaging Reporting and Data System in Diagnosing Focal Liver Lesions by Inexperienced Radiologists. *J Ultrasound Med* 2020;39:1537-1546.
131. Hussain SM, Terkivatan T, Zondervan PE, et al. Focal nodular hyperplasia: findings at state-of-the-art MR imaging, US, CT, and pathologic analysis. *Radiographics* 2004;24:3-17; discussion 18-19.
132. Burns PN, Wilson SR, Simpson DH. Pulse inversion imaging of liver blood flow: improved method for characterizing focal masses with microbubble contrast. *Invest Radiol* 2000;35:58-71.
133. Lee YS, Kim MJ, Han SW, et al. Superb microvascular imaging for the detection of parenchymal perfusion in normal and undescended testes in young children. *Eur J Radiol* 2016;85:649-656.
134. Sawatzki M. Diagnosis of typical nodular hyperplasia in the liver - use of a novel ultrasonic vascular Doppler technique. In: *UEGW. Wien: UEG Journal*; 2018:1.
135. Dietrich CF, Averkiou MA, Correas JM, Lassau N, Leen E, Piscaglia F. An EFSUMB introduction into Dynamic Contrast-Enhanced Ultrasound (DCE-US) for quantification of tumour perfusion. *Ultraschall Med* 2012;33:344-351.
136. Dong Y, Koch JBH, Lowe AL, et al. VueBox(R) for quantitative analysis of contrast-enhanced ultrasound in liver tumors. *Clin Hemorheol Microcirc* 2022;80:473-486.